Brain Stimulation 13 (2020) 1254–1262

Contents lists available at ScienceDirect

Brain Stimulation

journal homepage: http://www.journals.elsevier.com/brain-stimulation

Phase-specific manipulation of rhythmic brain activity by transcranial alternating current stimulation

Marina Fiene [a, *], Bettina C. Schwab [a], Jonas Misselhorn [a], Christoph S. Herrmann [b, c], Till R. Schneider [a], Andreas K. Engel [a]

[a] Department of Neurophysiology and Pathophysiology, University Medical Center Hamburg-Eppendorf, Hamburg, 20246, Germany
[b] Experimental Psychology Lab, Department of Psychology, Cluster of Excellence "Hearing4all", European Medical School, Carl von Ossietzky University Oldenburg, Oldenburg, 26129, Germany
[c] Research Center Neurosensory Science, Carl von Ossietzky University Oldenburg, Oldenburg, 26129, Germany

ARTICLE INFO

Article history:
Received 14 January 2020
Received in revised form
8 May 2020
Accepted 6 June 2020
Available online 10 June 2020

Keywords:
Transcranial alternating current stimulation
Electroencephalogram
Entrainment
Alpha oscillations
Visual flicker

ABSTRACT

Background: Oscillatory phase has been proposed as a key parameter defining the spatiotemporal structure of neural activity. To enhance our understanding of brain rhythms and improve clinical outcomes in pathological conditions, modulation of neural activity by transcranial alternating current stimulation (tACS) emerged as a promising approach. However, the phase-specificity of tACS effects in humans is still critically debated.
Objective: Here, we investigated the phase-specificity of tACS on visually evoked steady state responses (SSRs) in 24 healthy human participants.
Methods: We used an intermittent electrical stimulation protocol and assessed the influence of tACS on SSR amplitude in the interval immediately following tACS. A neural network model served to validate the plausibility of experimental findings.
Results: We observed a modulation of SSR amplitudes dependent on the phase shift between flicker and tACS. The tACS effect size was negatively correlated with the strength of flicker-evoked activity. Supported by simulations, data suggest that strong network synchronization limits further neuromodulation by tACS. Neural sources of phase-specific effects were localized in the parieto-occipital cortex within flicker-entrained regions. Importantly, the optimal phase shift between flicker and tACS associated with strongest SSRs was correlated with SSR phase delays in the tACS target region.
Conclusions: Overall, our data provide electrophysiological evidence for phase-specific modulations of rhythmic brain activity by tACS in humans. As the optimal timing of tACS application was dependent on cortical SSR phase delays, our data suggest that tACS effects were not mediated by retinal co-stimulation. These findings highlight the potential of tACS for controlled, phase-specific modulations of neural activity.

Introduction

Oscillations are a prominent feature of brain network dynamics proposed to be of particular importance for neural processing and, by extension, for normal and pathological brain function [1–4]. Modulation of such cortical activity by means of non-invasive brain stimulation represents a promising approach to advance knowledge on the functional role of the temporal patterning of neural activity and to improve clinical outcomes in disorders related to aberrant neural synchrony. Specifically, transcranial alternating current stimulation (tACS) is widely applied with the aim to entrain neural activity, assuming a periodic modulation of membrane potentials and a phase alignment of intrinsic oscillations to the tACS phase. This assumption is supported by studies in slice preparations and recordings in primates showing phase-specific modulations of neuronal spiking patterns by externally applied electric fields [5–8]. However, evidence from invasive recordings in animals may not directly be transferable to tACS effects in the human brain. Despite its broad use in basic and clinical science, the neural mechanism of tACS in humans is still under investigation and its overall efficacy has recently been challenged [9]. Measurements of

* Corresponding author. Department of Neurophysiology and Pathophysiology, University Medical Center Hamburg-Eppendorf, Martinistraße 52, 20246, Hamburg, Germany.
E-mail address: m.fiene@uke.de (M. Fiene).

https://doi.org/10.1016/j.brs.2020.06.008

the electric field strength in human cadaver brains and in epilepsy patients with implanted electrodes showed that most of the scalp-applied current is attenuated by skin and skull thereby questioning significant neural entrainment [9–11]. These findings, paralleled by inconsistent behavioral tACS effects [12–14], raised skepticism in the scientific community.

The theoretically ideal approach to counter this criticism by direct measurements of tACS-induced effects on neural activity in humans is currently not feasible due to strong and hard-to-predict electrical artifacts in concurrent recordings of extracellular potentials [15,16]. To provide evidence for acute phase-specific neuronal effects despite these methodological constraints, most studies assessed tACS effects on indirect measures assumed to be mediated by brain rhythms. For instance, tACS applied in the alpha and beta range was shown to lead to cyclic modulations of auditory, somatosensory or visual stimulus perception [17–20]. Further insight has been provided in the motor domain, by showing tACS-phase-dependent changes in cortical excitability [21–23] or peripheral tremor [24–26]. Yet, these prior conclusions only hold true under the assumption that the chosen outcome measures are reliable proxies for cortical rhythmic activity. The emergence of tremor, for instance, does not only rely on oscillatory cortical sources in the sensorimotor region but arises from complex information flow between cortex, cerebellum and thalamus [27]. Thus, direct electrophysiological evidence for phase-specific neuromodulation by tACS in humans is still missing.

Here, we used an innovative approach that combines rhythmic electrical with rhythmic sensory stimulation to test the phase-specificity of tACS. Via electroencephalography (EEG) we measured neural tACS effects on precisely controlled brain rhythms evoked by visual flicker, i.e., visually evoked steady state responses (SSRs), as a function of six phase shifts between tACS and flicker. Using an intermittent electrical stimulation protocol, concurrent 10 Hz flicker and multi-electrode tACS targeting the occipital cortex were applied in two sessions under active and sham tACS. Artifact free epochs in the interval immediately following tACS offset were used for SSR amplitude analysis (Fig. 1). We predicted that the amplitude of flicker-evoked rhythmic activity should be systematically modulated by the applied electric field dependent on the phase shift between flicker and tACS.

Materials and methods

Participants

24 healthy volunteers (mean age 25.1 ± 3.3 years; 16 female; 8 male; 22 right-handed) were recruited from the University Medical Center Hamburg-Eppendorf, Germany. The sample size was chosen based on the effect sizes between sham and active tACS in previous studies showing phase-dependent stimulation effects on sensory perception or peripheral tremor [18,24,28]. All participants reported normal or corrected-to-normal vision, no history of psychiatric or neurological disorders and were blind towards the tACS stimulation sequence. The experimental protocol was approved by the ethics committee of the Hamburg Medical Association and was conducted in accordance with the Declaration of Helsinki. All participants gave written informed consent before participation. Participants were monetarily compensated and debriefed immediately after the experiment.

Experimental design

All subjects participated in two separate sessions in a randomized, counterbalanced order under sham and active tACS. Participants were seated in a dimly lit, electrically shielded and sound-attenuated EEG chamber at a distance of approximately 40 cm to a white light emitting diode (LED). Prior to the main tACS block, 3 min eyes-open resting state EEG (RS_{pre}) was recorded while participants fixated the white illuminated LED. Afterwards, EEG during an 8 min SSR block without tACS (SSR_{pre}) was recorded. Single flicker periods (50 in total) were presented for 5.5 s followed by short breaks of 3–5 s. The timing of flicker presentation was identical to the procedure used in the main tACS block. In the tACS block, EEG was recorded continuously during the intermittent tACS protocol. Each trial started with tACS only and was followed by flicker onset after 3–5 s. The flicker continued until the end of the trial for 5.5 s in total. tACS free intervals of 2.5 s were used for EEG data analysis. Single tACS periods had a duration of 6–8 s. Between successive tACS epochs, tACS phase was continuous by adjusting only the amplitude but not the phase of the sine wave spanning the whole testing session. To account for the varying phase delay between neural activity induced by sensory and electrical stimulation, the visual flicker started at six different phase angles (0°, 60°, 120°, 180°, 240° and 300°) relative to the tACS cycle. 50 trials were recorded for each of the six phase shift conditions (300 trials in total). The sequence of trials was randomized such that every phase shift condition was followed equally likely by all other conditions. Moreover, to avoid confounding time-on-task effects on alpha amplitude, trials belonging to different conditions were evenly distributed over the course of the testing session by iterate permutation. The tACS block was divided in two blocks interrupted by a 10 min break. After the tACS block, another SSR block without tACS (SSR_{post}) and resting state EEG (RS_{post}) were recorded.

Transcranial stimulation

Multi-electrode tACS was applied via five additional Ag/AgCl electrodes (12 mm diameter) mounted between EEG electrodes. The montage was connected to a battery-driven current source (DC-Stimulator Plus, NeuroConn). After preparation with Signa electrolyte gel (Parker Laboratories Inc.), impedance of each outer electrode to the middle electrode was kept below 20 kΩ. Moreover, impedances were kept comparable to achieve an evenly distributed electric field. A sinusoidal alternating current of 2 mA peak-to-peak was applied at 10 Hz using an intermittent stimulation protocol. It has previously been shown that flicker-evoked SSRs show strongest amplitudes in the alpha frequency range [29]. Also, most reliable evidence for aftereffects of tACS on oscillatory power has been demonstrated in the alpha band that was proposed to result from neural phase alignment during stimulation [30,31]. Thus, we chose 10 Hz to test for the general feasibility of phase-specific effects by tACS, although our approach is not limited to this stimulation frequency. For sham stimulation, the current was ramped in and out over 15 s each. This procedure ensured that in both stimulation conditions, participants experienced initial skin sensations. During active stimulation, the current was ramped in over 15 s to 2 mA. After 90 s of continuous stimulation, tACS periods of 6–8 s without ramp were applied interrupted by short breaks of 2.5 s for EEG analysis. Total stimulation time during the active session was 40 min.

All participants confirmed that stimulation was acceptable and did not induce painful skin sensations. The most common side-effect was a tingling feeling on the scalp under the electrode. During the debriefing at the end of the final session, except for two subjects all participants correctly rated the sequence of active and sham stimulation. Further, no participant reported phosphene perception. This finding is in line with our simulation of the tACS-induced electric field which greatly diminishes with increasing distance to stimulation electrodes and is expected to be low in the retina [32].

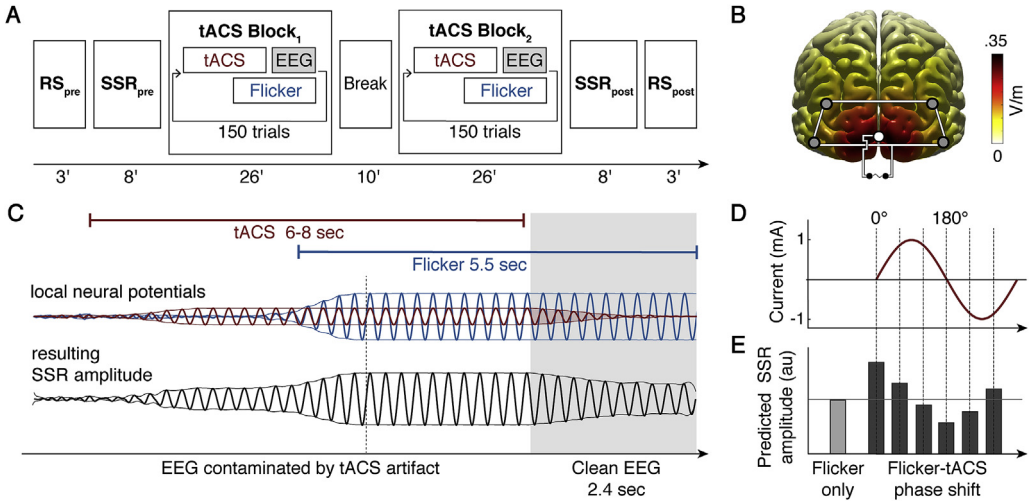

Fig. 1. Experimental setup. (A) Schematic display of the experimental timeline. The experiment was conducted on two separate days for active tACS and sham stimulation. Resting state (RS) and visually evoked steady state response (SSR) data without tACS were recorded pre and post to the tACS blocks. (B) tACS electrode montage and power of the tACS-induced stimulation field. The occipital electrode montage induced highest current densities over the primary visual cortex and current spread in surrounding areas. Maximum peak-to-peak difference in field strength was about 0.7 V/m (C) A schematic of the hypothesized effect of tACS on flicker-driven responses. Each trial started with tACS only, followed by flicker onset after 3–5 s. The flicker continued for 5.5 s until the end of the trial. Flicker and tACS induce phase alignment of neural activity as illustrated for local neural potentials that can outlast the stimulation period for a few cycles after stimulation offset (red-shaded tACS entrainment echo). If voltage modulations by tACS and flicker interact in a phase-specific manner, SSRs should reflect this interaction in net amplitude modulations of the scalp electroencephalogram (EEG). The gray-shaded intervals were used for tACS artifact-free EEG data analysis. (D) To vary the phase between neural activity induced by electrical and sensory rhythmic stimulation, visual flicker started at six different phase shifts relative to the tACS cycle. 50 trials per phase angle were presented in randomized order. (E) Predicted enhancement and suppression of net SSR amplitudes based on the phase-shift between flicker and tACS.

Electrophysiological recording

EEG was recorded continuously from 64 Ag/AgCl electrodes (12 mm diameter) mounted in an elastic cap (Easycap). The electrooculogram was recorded from two electrodes placed below both eyes with the EEG referenced to the nose tip. Electrodes were prepared with abrasive conducting gel (Abralyt 2000, Easycap) keeping impedance below 20 kΩ. EEG data were recorded using BrainAmp DC amplifiers (Brain Products GmbH) and the corresponding software (Brain Products GmbH, Recorder 1.20). Data were recorded with an online passband of 0.016–250 Hz and digitized with a sampling rate of 1000 Hz.

Data analysis

EEG spectral analysis was performed on sensor and source level. We expected to find phase-specific tACS-induced modulations of SSR amplitude at electrode positions showing prominent phase alignment to flicker stimulation. Therefore, we assessed the spatial distribution of phase locking values (PLVs) between EEG and visual flicker in the SSR_{pre} blocks without tACS (see Supplementary Material A).

For analysis of SSR amplitude modulation during the tACS block, we computed the Fourier transform of each trial separately for the time epochs of 0.1–1.1 s, 0.6–1.6 s and 1.1–2.1 s after tACS offset. The first 0.1 s after stimulation offset were rejected before EEG data filtering to avoid smearing of initial tACS artifacts into the analysis time window. A thorough tACS artifact correction procedure was applied to prevent leakage of electrical artifacts into the stimulation-free epochs as described in detail in Supplementary Material A. To correct for global alpha amplitude fluctuations over time independent of experimental manipulation, SSR amplitude was defined as a relative amplitude value by subtracting the mean amplitude at neighboring frequencies (9 and 11 Hz) from the absolute amplitude at the stimulation frequency.

For the assessment of SSR amplitude modulation dependent on the relative phase shift between tACS and flicker, bar diagrams were constructed showing the variation in SSR amplitude over phase shift conditions. SSR amplitude was normalized by the sum of amplitude values over all six conditions. Assignment of trials to phase conditions for the sham session was performed using the same trial numbers as under tACS stimulation, thereby ensuring equal time-on-task effects for both sessions. Amplitude modulation was assessed via three modulation measures. First, we calculated the Kullback-Leibler divergence (D_{KL}), measuring the deviation of the observed amplitude distribution P from a uniform distribution U defined as

$$D_{KL}(P,U) = \sum_{i=1}^{N} P(i)\ log\left[\frac{P(i)}{U(i)}\right] \quad (1)$$

where N is the number of phase bins [33]. Strict uniformly distributed amplitude values would be reflected in $D_{KL} = 0$ whereas D_{KL} increases the further away P gets from U. Second, we assessed whether the tACS-induced amplitude modulation over phase conditions follows a cyclic pattern, as hypothesized based on the sinusoidal nature of tACS. Therefore, we calculated the locking of amplitude values to phase condition (amplitude phase locking, APL) defined as

$$APL = \left|\frac{1}{b}\sum_{b} A_b\ e^{i\theta_b}\right| \quad (2)$$

where A and θ are the normalized relative amplitude and phase shift for each of the six phase shift conditions b. Third, to further investigate whether the tACS-induced SSR amplitude modulation can be described by a sinusoidal pattern, we fitted one-cycle sine waves to SSR amplitude bar diagram values [18,34]. Thus, while D_{KL} describes a general modulation of SSR amplitudes, APL and sine fit assess systematic, phase-dependent modulation patterns.

For each of the three modulation indices, we calculated dependent samples t-tests for the three time epochs after tACS offset between sham and active tACS on sensor level. Effect sizes were determined by calculating Cohen's d_z for paired t-test comparisons. To account for comparisons in multiple time windows, we applied Bonferroni correction to the significance level and report test statistics if the corresponding p-value fell below the corrected alpha of $\alpha_{bonf} = .0167$ (= .05/3). For source localization of tACS effects, neural activity was estimated using exact low resolution brain electromagnetic tomography (eLORETA) [35]. We analyzed the APL parameter resulting from the epoch immediately following tACS offset in source space and computed dependent samples t-tests at each grid point using cluster-based permutation tests. Finally, we checked for a potential SSR modulation by electrical co-stimulation of the retina, in which case the individual cortical SSR phase delay relative to flicker should have no predictive value for the optimal flicker-tACS phase shift leading to SSR enhancement. Accordingly, the dependency of optimal flicker-tACS phase shifts on the cortical flicker-SSR phase delays was examined by computing circular-circular correlations per channel using cluster-based permutation tests [36]. For a detailed description of spectral and statistical data analyses see Supplementary Material A.

Results

Flicker-evoked neural phase alignment in the parieto-occipital cortex

To analyze sensory entrainment by visual flicker, we assessed the degree and spatial distribution of phase locking between EEG and 10 Hz flicker stimulation. Estimated time series on source level displayed a prominent peak of parieto-occipital EEG-flicker PLV (Fig. 2B). Strong phase locking was located in the superior and middle occipital gyrus as well as in bilateral precuneus and cuneus. According to our hypothesis of sensory-electric interaction that requires sufficiently high phase-consistency of the targeted rhythm, we selected electrodes with mean PLV > 0.5 for the analysis of phase-specific SSR amplitude modulation by tACS. Mean PLV for the four selected channels (corresponding to electrodes O1, O2, POz, Pz) during both SSR_{pre} blocks over all participants was 0.56 ± 0.16 (mean ± sd). As illustrated in the lower part of Fig. 2B, data showed varying phase delays between flicker and cortical SSR across participants, likely originating from individual delays in neural propagation of SSRs and individual anatomy. Further, spectra revealed an amplitude increase at the flicker stimulation frequency compared to resting state ($t(23) = 6.99$, $p < .001$, $d_z = 1.43$; Fig. 2C). Between-subject correlation showed that the strength of EEG-flicker phase locking was positively correlated with the increase in SSR amplitude from resting state to flicker stimulation in SSR_{pre} blocks ($r = .42$, $p = .039$) (Fig. 2D).

Phase-dependent amplitude modulation of flicker-evoked activity by tACS

To test the hypothesis that simultaneous tACS and flicker stimulation lead to phase-specific interactions between sensory-evoked neural activity and tACS electric field, we assessed differences in SSR amplitudes between tACS phase conditions. Fig. 3A depicts normalized SSR amplitude bar diagrams over the six phase shift conditions for two exemplary participants. During sham, the data showed small fluctuations in SSR amplitude with no preference for a particular phase shift condition. In contrast, active stimulation led to phase-dependent modulations of SSR amplitudes indicating an interaction between tACS-induced electric field and flicker-evoked rhythmic activity. The degree of tACS-phase-

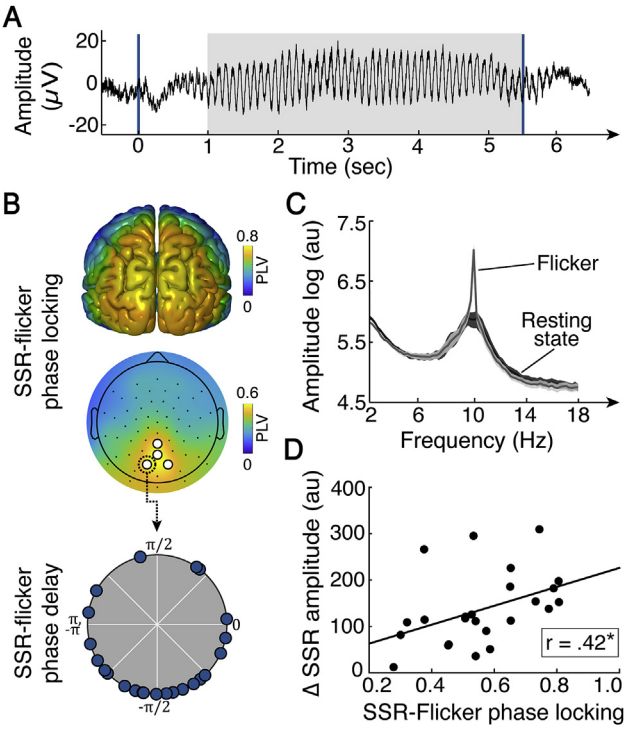

Fig. 2. Phase locking values (PLVs) of steady state responses (SSRs) to flicker over all trials of the active and sham SSR_{pre} blocks. (A) SSR during 5.5 s flicker stimulation computed as the average of 50 raw EEG traces of one exemplary participant at channel POz. Blue lines mark the onset and offset of visual flicker. The gray-shaded area depicts the time window used for EEG data analysis. (B) Source and sensor level spatial distribution of mean PLVs over all participants with maximal phase locking over the parieto-occipital cortex. Markers correspond to channels selected on sensor level for SSR amplitude analysis. The lower part shows the interindividual variation in phase delays between flicker and resulting cortical SSR exemplary for electrode O1. (C) Mean amplitude spectrum during flicker stimulation and resting state over all participants for the four selected channels on sensor level. Shaded areas indicate the standard error of the mean. (D) The strength of SSR-flicker phase locking at the four parieto-occipital channels is positively correlated with the increase in SSR amplitude from resting state to SSR_{pre} blocks across participants ($r = .42$, $p = .039$, $n = 24$). *$p < .05$.

dependence of SSR amplitude was quantified via three different modulation measures: (1) Kullback-Leibler divergence (D_{KL}), measuring the deviation of amplitude values from a uniform distribution, (2) the locking of amplitude values to phase conditions (APL) and (3) one-cycle sine fit to SSR amplitude values. We compared these measures between tACS and sham for time windows directly following tACS offset (0.1–1.1 s) and with some delay (0.6–1.6 s and 1.1–2.1 s).

Immediately after tACS offset, SSR amplitude distributions deviated significantly stronger from uniform distribution as quantified by D_{KL} compared to sham ($t(23) = 3.26$, $p = .003 < \alpha_{bonf}$, $d_z = 0.67$; Fig. 3B). Phase locking of amplitude values to phase condition measured by APL was significantly larger after tACS ($t(23) = 3.06$, $p = .005 < \alpha_{bonf}$, $d_z = 0.63$). Similarly, also the one-cycle sine wave fit to SSR amplitudes showed a significantly greater amplitude of the sine fit under tACS ($t(23) = 3.58$, $p = .002 < \alpha_{bonf}$, $d_z = 0.73$; Fig. 3B). The proportion of explained variance R^2 by sine fit was greater for SSR amplitude modulation under tACS compared to sham ($t(23) = 2.52$, $p = .019$, $d_z = 0.52$). In successive time windows, the modulatory tACS effect decayed for all three modulation parameters (Fig. 3E and Supplementary Material B, Table B1).

In order to test whether this modulatory effect was mediated by the overall amplitude or variability of alpha activity, we compared

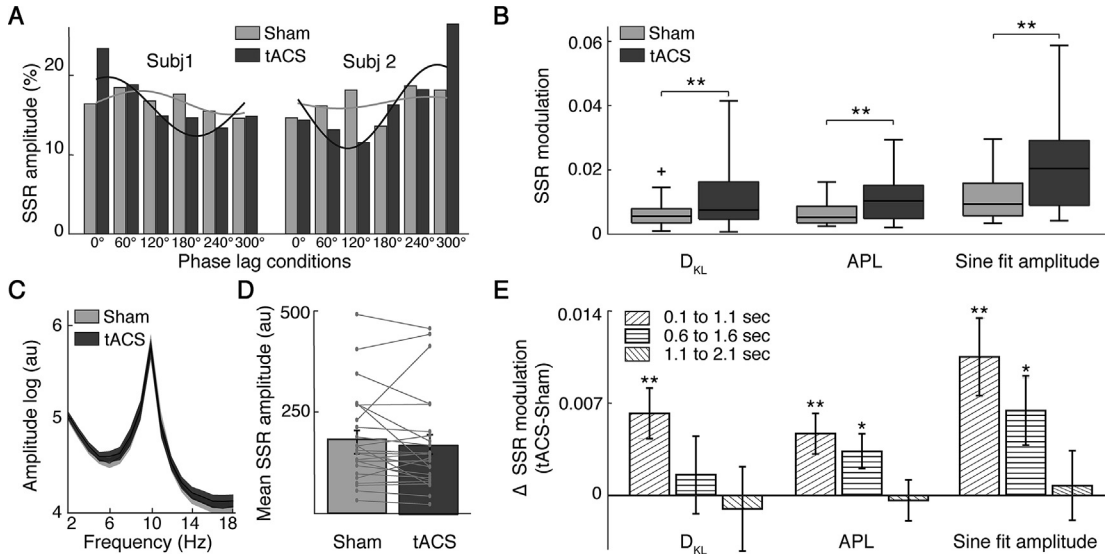

Fig. 3. Steady state response (SSR) amplitude modulation by tACS for the time window of 0.1–1.1 s after stimulation offset during the tACS block on sensor level. (A) SSR amplitude bar graphs for two exemplary participants. SSR amplitude values differ in the degree of phase dependence under tACS compared to sham. Inserted lines show sinusoidal fits to the data. (B) Significantly increased Kullback-Leibler divergence (D_{KL}), enhanced phase locking of amplitude values to phase condition (APL) and sine fit amplitudes under tACS relative to sham. (C, D) Phase-dependent amplitude modulation is not paralleled by differences in mean absolute 10 Hz alpha amplitude or mean SSR amplitude over all trials and participants between stimulation conditions. Shaded areas and error bars indicate the standard error of the mean. (E) Decay in tACS effect size over three time windows after tACS offset. Bar graphs show the mean difference in SSR amplitude modulation between active and sham tACS condition quantified via three modulation measures. Asterisks mark the uncorrected *p*-value of dependent samples t-tests. Only statistical tests for the first 1 s time epoch after tACS offset remain significant after Bonferroni correction for comparisons in multiple time windows ($\alpha_{bonf} = 0.0167$; 0.05/3). Error bars represent the standard error. *$p < .05$; **$p < .01$.

mean SSR amplitude, mean absolute 10 Hz amplitude and standard deviation of SSR amplitudes in the first epoch after tACS offset between sham and tACS condition. None of these comparisons yielded significant differences (SSR amplitude: $t(23) = -1.01$, $p = .321$, $d_z = -0.21$; Fig. 3D; absolute 10 Hz alpha amplitude: $t(23) = -.94$, $p = .36$, $d_z = -0.19$; Fig. 3C; standard deviation of SSR amplitudes: $t(23) = -.30$, $p = .767$, $d_z = -0.06$; see also Supplementary Material B, Table B2). Taken together, data implies a strengthening and dampening of SSR amplitudes dependent on the phase shift between tACS and flicker stimulation.

Spatial localization and dependency of tACS effects on individual physiology

The spatial specificity of tACS effects was analyzed in source space for the APL modulation parameter. Compared to D_{KL}, APL is a more specific index assuming systematic amplitude modulations by tACS. Moreover, its computation is more stable compared to the sine fit as no assumptions about parameter ranges are required. Cluster analysis in source space showed significantly increased SSR amplitude modulation quantified by APL during active tACS relative to sham in a cluster over the parieto-occipital cortex (cluster test: $p = .004$; Fig. 4A). Significant differences were located primarily in the bilateral precuneus, superior parietal gyrus and midcingulate area as well as the cuneus and calcarine sulcus. These were part of flicker-entrained brain areas, located in tACS-targeted cortical regions and connected higher visual areas (cf. Fig. 2B). Cluster analysis on sensor level confirmed significant SSR modulation at the four channels selected for sensor level analysis and at channels Iz, CPz and P1 (cluster test: $p = .011$). Interestingly, visual inspection of source localization suggests that tACS effects on SSR amplitude were weaker in the middle and superior occipital gyrus, where neural phase alignment to the visual flicker was dominant, and were stronger in neighboring occipital and parietal regions.

In accordance with this finding, we further observed a highly significant between-subject correlation of SSR amplitude modulation quantified by APL with the underlying strength of EEG-flicker phase locking during active tACS on sensor level ($r = -.66$, $p < .001$). Participants with strong neural synchronization by flicker showed weaker SSR amplitude modulation by tACS (Fig. 4B). This relation was non-significant during the sham session ($r = -.38$, $p = .067$). To test that stronger phase locking is not generally associated with less amplitude variation and, thus, weaker APL values, we computed the correlation between the differences in PLVs with corresponding differences in APL values between sham and tACS condition. The Pearson correlation coefficient was not significant ($r = -.31$, $p = .143$), suggesting that the strong negative relation between SSR-flicker phase locking and SSR modulation is specific for tACS-induced neuromodulation. Our results, thus, emphasize the impact of the individual physiology, influenced by the neuronal response strength to visual flicker, for the detection of neural tACS effects. The negative correlation further suggests the existence of ceiling effects in tACS neuromodulation, with tACS effects being limited when neural activity at the stimulation frequency was highly synchronous, i.e., when the network was already optimally driven.

In order to gain mechanistic insight into the relation between flicker-evoked synchronization and tACS effect size, we simulated a spiking network model of 1000 randomly connected neurons. Excitatory and inhibitory neurons were described by the model of Izhikevich [37] and network activity was tuned to an alpha oscillation by adapting parameters of an existing network model [38]. A detailed description of the model parameters is given in Supplementary Material A. To simulate flicker and tACS effects on neural spiking activity, two sinusoidal inputs with systematic phase shift were added. The amplitude of flicker input was ten times larger compared to the tACS input. The proportion of excitatory neurons receiving flicker sine input was logarithmically increased from 0 to 100% to simulate varying strengths of flicker-evoked synchronization in the network, while tACS sine input was given to all excitatory neurons. Fig. 3C depicts normalized SSR amplitude values dependent on the six flicker-tACS phase shifts and the proportion of neurons driven by flicker input. In the absence of flicker input, there was no evoked

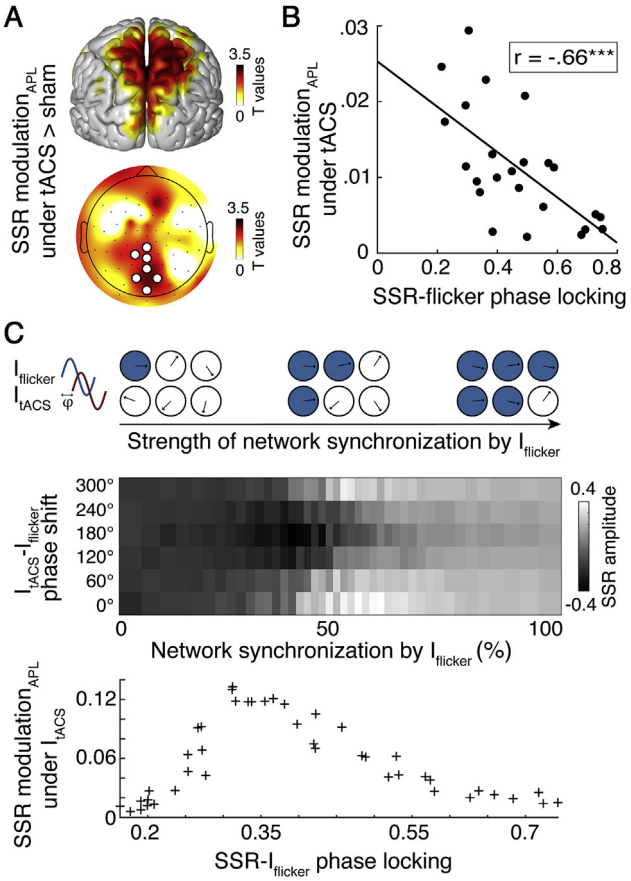

Fig. 4. Steady state response (SSR) amplitude modulation across flicker-tACS phase shifts quantified by amplitude phase locking (APL) during the first 1 s epoch after tACS. (A) Source and sensor level analysis of differences in SSR modulation quantified by APL between active and sham tACS show significant clusters over the parieto-occipital cortex. (B) On sensor level, between-subject correlation shows that the tACS effect size quantified via APL is negatively related to EEG-flicker phase locking during the tACS block (r = -.66, p < .001, n = 24). (C) Neural network simulation on the relation between tACS effect size and the strength of flicker-evoked network synchronization. Neurons were driven by two sinusoidal inputs, $I_{flicker}$ and I_{tACS}, at six phase shifts. Only for intermediate flicker-driven network synchronization strengths, data show systematic modulations of normalized SSR amplitudes dependent on the relative phase-shift between flicker and tACS. With further increasing flicker-evoked network synchronization, a successively larger proportion of neurons is phase-locked to the flicker input, being less susceptible to weak tACS inputs. The corresponding decline in APL values matches the observed negative correlation in our experimental dataset. ***p < .001.

neuronal phase alignment that could interact with tACS effects, resulting in APL values at noise level. For intermediate network synchronization with PLV of 0.3, tACS input showed clear phase-specific modulatory effects on SSR amplitude which declined when flicker-evoked synchronization was further increased in the network. This simulation result resembles the negative correlation between tACS effect size and SSR-flicker phase locking in our experimental dataset. Thus, our simulations suggest that phase-dependent interactions between SSR and tACS effects are only observable if phase locking to flicker is present, yet, dominant flicker-evoked network synchronization can limit further neuromodulation by tACS.

tACS effects were not mediated by retinal stimulation

To examine the potential involvement of electrical co-stimulation of the retina on SSR amplitude modulation, we analyzed the dependency of optimal flicker-tACS phase shifts associated with strongest SSR enhancement on individual flicker-SSR phase delays in the visual cortex. Assuming an interaction between flicker and electric field at the retinal level, the neural phase delay of the cortical SSR should have no predictive value for the optimal timing of tACS application. Notably, only during active tACS, permutation tests revealed a significant cluster of occipital electrodes (O1, O2, O9, O10; cluster test: p = .009) showing a circular correlation between SSR phase delay and optimal flicker-tACS phase shift across participants (Fig. 5). The mean correlation coefficient across cluster electrodes was r = -.54. Corresponding permutation tests during sham showed no significant electrode cluster. This implies that the interaction between flicker-evoked responses and tACS effects was unlikely to be caused by retinal co-stimulation.

Discussion

We used an innovative approach to study the phase-specificity of tACS effects in humans by systematically pairing rhythmic electrical with rhythmic visual stimulation. Using EEG, we evaluated the amplitude of flicker-evoked SSRs in the interval immediately following tACS delivered at six different phase shifts relative to flicker. We demonstrate that SSR amplitudes are modulated in a tACS phase-dependent manner, leading to both enhancement and suppression of visually evoked activity. The individual phase delay between flicker and cortical SSR is predictive of the optimal timing of tACS application. Interestingly, tACS effect size is limited by the strength of the underlying flicker-evoked network synchronization, pointing to ceiling effects in tACS effectiveness. The plausibility of such ceiling effects is demonstrated by simulations of a spiking network model.

Previous investigations into the tACS mechanism of action typically aimed to modulate ongoing or task-related brain oscillations which show high variability in frequency and phase consistency. Here, we used SSRs that allow the precise setting of the neural waveform in the visual cortex. While the mechanism underlying SSR generation is being debated, increasing evidence supports the involvement of entrained endogenous oscillations in the processing of rhythmic visual input [39–41]. Yet, irrespective of their exact physiological origin, SSRs can be treated as stimulus-driven brain rhythms with predictable time course, which enables a highly specific targeting by tACS. Notably, compared to ongoing activity, the phase of the SSR is not expected to be shifted by tACS as EEG recordings will always show dominant phase locking to the driving flicker. Rather, if neural activity related to electrical and sensory stimulation interact in a phase-specific manner, SSRs should reflect this interaction in net amplitude modulations. Our data confirmed that SSR amplitudes measured immediately after tACS offset are dependent on the relative phase shift between flicker and tACS. Importantly, as data show no overall amplitude increase of SSRs by tACS (Fig. 3D), results imply a phase-dependent enhancement and suppression of flicker responses. This is in accordance with recent invasive recordings in animals, showing that tACS modulates neuronal spike timing rather than spike rate [7,8]. Thus, our data provide the first conclusive evidence for the phase-specificity of tACS effects in human electrophysiological recordings.

The phase-dependent modulation of SSR amplitude was robust under three modulation measures but already decayed during the first 2 s after tACS offset. While lasting power enhancement after prolonged alpha tACS has been repeatedly shown and ascribed to synaptic plasticity mechanisms [30,31,42], evidence for outlasting effects on phase synchronization is still sparse. Yet, neural oscillatory activity entrained during rhythmic electric, magnetic or visual stimulation were shown to remain stable for a few cycles after

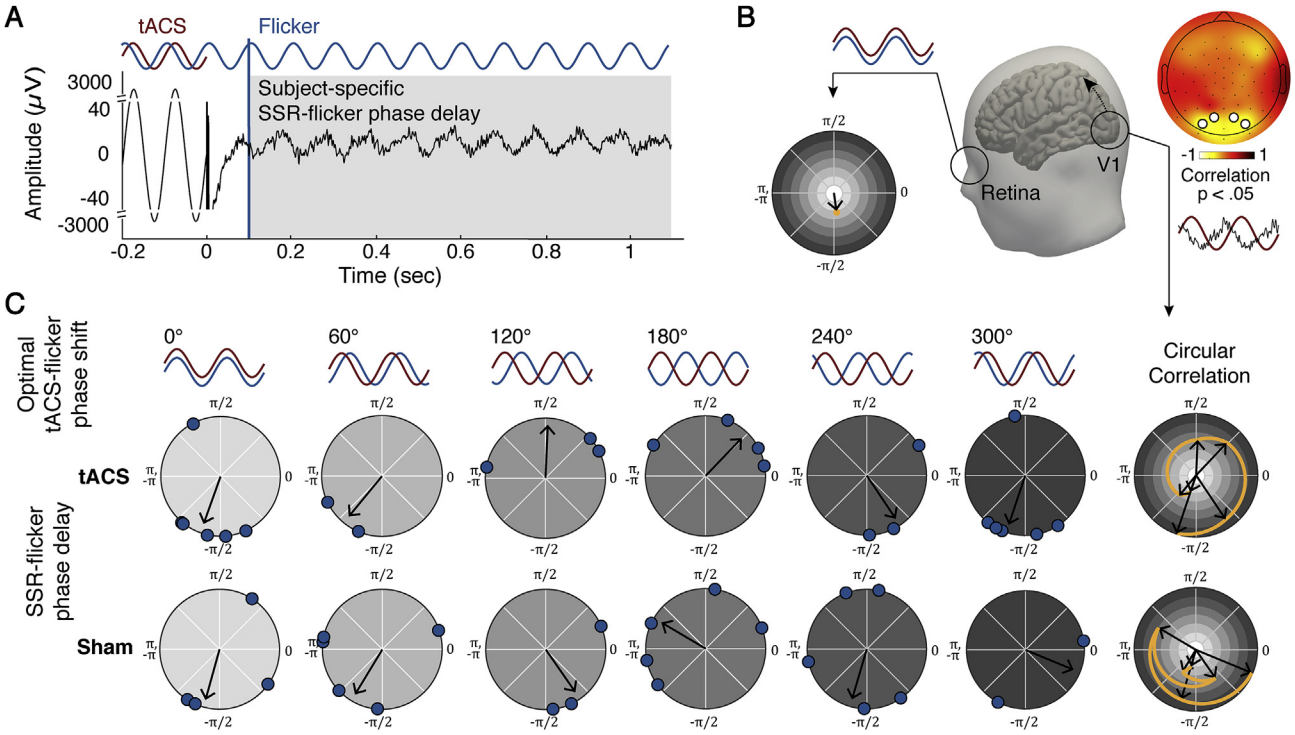

Fig. 5. Relationship between the cortical steady state response (SSR) phase delay relative to flicker and the optimal timing of tACS application associated with strongest SSRs. (A) Raw EEG data during the tACS block of one representative participant at electrode O1. Data during the last 0.2 s of tACS stimulation show strong electrical artifacts. The gray-shaded area depicts the time window used for data analysis. (B) In case of an interference of flicker and electric field in the retina, the optimal flicker-tACS phase shift should be independent of individual cortical SSR phase delays and be comparable across participants as exemplified in the polar plot. In contrast, a significant cluster of occipital electrodes reveals a circular correlation between optimal flicker-tACS phase shift and subject-specific SSR phase delays only during the tACS session. This suggests an interaction of tACS effects and SSR at early stages of visual cortical processing with concurrent spread of activity to higher visual areas. (C) Polar plots show flicker-SSR phase delays for all participants grouped by optimal flicker-tACS phase shift conditions exemplary for electrode O1. Blue circles show the mean flicker-SSR phase delay computed over all trials per participant and arrows depict the mean phase angle over all trials per optimal flicker-tACS phase shift condition. Circular plots on the right summarize the course of the mean flicker-SSR phase angles over the six flicker-tACS phase shift conditions (gray color code corresponds to flicker-tACS phase shifts of preceding polar plots). During tACS, the data show a significant circular correlation between individual SSR phase delays and optimal flicker-tACS phase shifts across participants. There is no significant circular correlation during the sham session.

stimulation offset [43–45]. These short-lived reverberations of oscillatory activity, phase-locked to the external force, have been termed entrainment echoes [44,46]. Notably, Vossen et al. [30] could not find evidence for entrainment echoes after short tACS epochs of 3 or 8 s length. However, while tACS phase effects might not be detectable as prolonged phase locking in ongoing brain activity, flicker-induced brain rhythms may increase the signal-to-noise ratio and thereby enhance the detectability of short-lived tACS aftereffects. Our results are compatible with the assumption of tACS-induced entrainment of neural activity, which yet cannot be tested directly due to artifact-contaminated EEG recordings. We speculate that the observed effects generalize to tACS and SSRs in other frequency bands of the human EEG, which should be systematically investigated in future studies.

Interestingly, the efficacy of tACS was inversely related to the strength of the underlying flicker response. More precisely, tACS-induced SSR amplitude modulation was limited in participants showing highest network synchronization by visual flicker. It has repeatedly been demonstrated that tACS effect sizes are related to the baseline level of oscillatory activity, with effects only being measurable when power at the stimulated frequency was low [47–49]. Similarly, our data indicate that in participants and anatomical regions exhibiting strong EEG-flicker phase locking, dominant synchronous neural activity was less prone to the effect of tACS. Our simulation of a simple network model of spiking neurons reveals a possible mechanism for this effect. While network synchronization by flicker is the prerequisite for phase-dependent interactions between flicker-evoked activity and tACS effects, dominant entrainment in an increasing number of neurons by a relatively strong driving force (i.e., flicker) might limit susceptibility for entrainment to the weaker source (i.e., tACS).

An important consideration for the interpretation of tACS effects is the possible involvement of peripheral sensory co-stimulation that may indirectly lead to neural entrainment. First, electric stimulation of peripheral nerves in the skin can induce rhythmic activation of the somatosensory cortex. While somatosensory entrainment has been shown to at least partly explain tACS effects on motor cortex [50], recent studies demonstrated that tACS affects neural activity even if somatosensory input is controlled for [7,51]. Thus, tACS can exert its effect via direct transcranial as well as indirect somatosensory entrainment, and both can theoretically contribute to physiological modulations depending on the stimulation protocol. The close link between motor and somatosensory regions may explain the predominance of cutaneous co-stimulation effects when targeting the motor cortex. Yet, evidence for the spatial specificity of occipital or fronto-occipital tACS effects by the use of active control montages support a predominant transcranial mechanism of action in these studies [7,52]. In our data, the dependency of tACS effects on the SSR phase delay over the primary visual cortex, i.e., the target region of the electrical stimulation, may support transcranial stimulation effects on SSR at early stages of visual cortical processing with concurrent spread of activity to higher visual areas, likely via polysynaptic interactions along the visual stream [53–55]. However, to rule out entirely that SSRs were influenced by somatosensory co-stimulation, a control electrode montage would be necessary that elicits equivalent tactile

sensation without stimulating the cortex. This is challenging as cutaneous stimulation effects may not only depend on current strength but also on the distribution and sensitivity of skin receptors and cranial nerves in the stimulated area [56]. Therefore, the development of valid control montages is one of the key goals in future tACS research.

Second, it has been noted that tACS can cause activation of the retinae due to shunting of scalp-applied currents across the skin. Although no participant reported phosphene sensation with the used focal ring montage, sub-threshold activation of the retinae could in principle have an impact on visual processing, which was previously dealt with by using control electrode montages [56]. Here, our experimental approach allowed to directly investigate the influence of retinal stimulation effects. It is well documented that flicker stimulation will inevitably lead to variable phase delays in the recordable SSR [57,58]. Accordingly, a cortical interaction between tACS effects and SSRs should be associated with varying optimal phase shifts between tACS and flicker across participants. This was exemplified in a study by Ruhnau et al. [59], showing that simultaneously started tACS and flicker did not lead to tACS-induced power increases of the fundamental SSR component in the overall sample. In our study, we could show that the optimal flicker-tACS phase shift associated with strongest SSRs was correlated with the individual flicker-SSR phase delay over the primary visual cortex. This finding suggests that it is possible to predict the optimal timing of tACS application based on the subject-specific neural phase of the cortical SSR. Importantly, this dependency cannot be explained by an interference between flicker and electric field at the retinal level, which should be independent of post-retinal neural processing and, therefore, result in comparable optimal flicker-tACS phase shifts across participants. Thus, our finding strongly suggests that the interaction between tACS effect and SSR was not mediated by retinal co-stimulation.

In conclusion, we provide the first conclusive electrophysiological evidence for the efficacy of tACS to modulate rhythmic cortical activity in a phase-dependent manner in humans. Importantly, we found that the optimal phase shift between electrical and visual stimulation varies between participants and depends on the neural phase delay of the visual response in the tACS target region. This result cannot be explained by peripheral electrical co-stimulation of the retina. Furthermore, our data corroborate the notion that tACS effect size is limited by the strength of the targeted oscillatory activity level. Taken together, our findings show that individual functional properties and the current brain state need to be considered to achieve specific, custom-fit neuromodulation. In the context of the ongoing debate on the overall capability of tACS to entrain neural activity in humans, our results make a strong case for its periodic impact on neuronal excitability that would allow for frequency- and phase-specific modulations of brain signals.

Declaration of competing interest

None.

CRediT authorship contribution statement

Marina Fiene: Conceptualization, Methodology, Investigation, Formal analysis, Writing - original draft, Visualization. **Bettina C. Schwab:** Conceptualization, Methodology, Writing - review & editing, Supervision. **Jonas Misselhorn:** Conceptualization, Methodology, Writing - review & editing. **Christoph S. Herrmann:** Conceptualization, Methodology, Writing - review & editing. **Till R. Schneider:** Conceptualization, Methodology, Writing - review & editing, Funding acquisition. **Andreas K. Engel:** Conceptualization, Methodology, Writing - review & editing, Funding acquisition, Project administration.

Acknowledgements

This work was supported by the Deutsche Forschungsgemeinschaft (SFB 936/A3 awarded to A.K.E. and T.R.S.; SPP 1665/EN 533/13-1 and SFB TRR 169/B1 awarded to A.K.E.; SPP 1665/SCHN 1511/1–2 awarded to T.R.S.) and by the Studienstiftung des deutschen Volkes (awarded to M.F.). We thank Jonathan Daume, Alexander Maye, Jan-Ole Radecke and Darius Zokai for helpful discussions on the data, Malte Sengelmann and Guido Nolte for methodological support, and Karin Deazle and Darius Zokai for assistance in data recording.

Appendix A. Supplementary data

Supplementary data to this article can be found online at https://doi.org/10.1016/j.brs.2020.06.008.

References

[1] Fries P. A mechanism for cognitive dynamics: neuronal communication through neuronal coherence. Trends Cognit Sci 2005;9:474–80. https://doi.org/10.1016/j.tics.2005.08.011.
[2] Schnitzler A, Gross J. Normal and pathological oscillatory communication in the brain. Nat Rev Neurosci 2005;6:285–96. https://doi.org/10.1038/nrn1650.
[3] Ronconi L, Melcher D. The role of oscillatory phase in determining the temporal organization of perception: evidence from sensory entrainment. J Neurosci 2017;37:10636–44. https://doi.org/10.1523/JNEUROSCI.1704-17.2017.
[4] Engel AK, Fries P, Singer W. Dynamic predictions: oscillations and synchrony in top–down processing. Nat Rev Neurosci 2001;2:704–16. https://doi.org/10.1038/35094565.
[5] Ali MM, Sellers KK, Fröhlich F. Transcranial alternating current stimulation modulates large-scale cortical network activity by network resonance. J Neurosci 2013;33:11262–75. https://doi.org/10.1523/JNEUROSCI.5867-12.2013.
[6] Reato D, Rahman A, Bikson M, Parra LC. Effects of weak transcranial alternating current stimulation on brain activity—a review of known mechanisms from animal studies. Front Hum Neurosci 2013;7:687. https://doi.org/10.3389/fnhum.2013.00687.
[7] Krause MR, Vieira PG, Csorba BA, Pilly PK, Pack CC. Transcranial alternating current stimulation entrains single-neuron activity in the primate brain. Proc Natl Acad Sci Unit States Am 2019:201815958. https://doi.org/10.1073/pnas.1815958116.
[8] Johnson L, Alekseichuk I, Krieg J, Doyle A, Yu Y, Vitek J, et al. Dose-dependent effects of transcranial alternating current stimulation on spike timing in awake nonhuman primates. BioRxiv 2019:696344. https://doi.org/10.1101/696344.
[9] Underwood E. Cadaver study challenges brain stimulation methods. Science 2016;352. https://doi.org/10.1126/science.352.6284.397. 397–397.
[10] Vöröslakos M, Takeuchi Y, Brinyiczki K, Zombori T, Oliva A, Fernández-Ruiz A, et al. Direct effects of transcranial electric stimulation on brain circuits in rats and humans. Nat Commun 2018;9:483. https://doi.org/10.1038/s41467-018-02928-3.
[11] Huang Y, Liu AA, Lafon B, Friedman D, Dayan M, Wang X, et al. Measurements and models of electric fields in the in vivo human brain during transcranial electric stimulation. Elife 2017;6:1–26. https://doi.org/10.7554/eLife.18834.
[12] Brignani D, Ruzzoli M, Mauri P, Miniussi C. Is transcranial alternating current stimulation effective in modulating brain oscillations? PloS One 2013;8:e56589. https://doi.org/10.1371/journal.pone.0056589.
[13] Fekete T, Nikolaev AR, De Knijf F, Zharikova A, van Leeuwen C. Multi-electrode alpha tACS during varying background tasks fails to modulate subsequent alpha power. Front Neurosci 2018;12:428. https://doi.org/10.3389/fnins.2018.00428.
[14] Vossen A. Modulation of neural oscillations and associated behaviour by transcranial alternating current stimulation (tACS). 2017. PhD thesis.
[15] Noury N, Hipp JF, Siegel M. Physiological processes non-linearly affect electrophysiological recordings during transcranial electric stimulation. Neuroimage 2016;140:99–109. https://doi.org/10.1016/j.neuroimage.2016.03.065.
[16] Noury N, Siegel M. Phase properties of transcranial electrical stimulation artifacts in electrophysiological recordings. Neuroimage 2017;158:406–16. https://doi.org/10.1016/j.neuroimage.2017.07.010.
[17] Gundlach C, Müller MM, Nierhaus T, Villringer A, Sehm B. Phasic modulation of human somatosensory perception by transcranially applied oscillating currents. Brain Stimul. 2016;9:712–9. https://doi.org/10.1016/j.brs.2016.04.014.

[18] Neuling T, Rach S, Wagner S, Wolters CH, Herrmann CS. Good vibrations: oscillatory phase shapes perception. Neuroimage 2012;63:771–8. https://doi.org/10.1016/j.neuroimage.2012.07.024.
[19] Helfrich RF, Schneider TR, Rach S, Trautmann-Lengsfeld SA, Engel AK, Herrmann CS. Entrainment of brain oscillations by transcranial alternating current stimulation. Curr Biol 2014;24:333–9. https://doi.org/10.1016/j.cub.2013.12.041.
[20] Riecke L, Formisano E, Herrmann CS, Sack AT. 4-Hz transcranial alternating current stimulation phase modulates hearing. Brain Stimul. 2015;8:777–83. https://doi.org/10.1016/j.brs.2015.04.004.
[21] Nakazono H, Ogata K, Kuroda T, Tobimatsu S. Phase and frequency-dependent effects of transcranial alternating current stimulation on motor cortical excitability. PloS One 2016;11:e0162521. https://doi.org/10.1371/journal.pone.0162521.
[22] Guerra A, Pogosyan A, Nowak M, Tan H, Ferreri F, Di Lazzaro V, et al. Phase dependency of the human primary motor cortex and cholinergic inhibition cancelation during beta tACS. Cerebr Cortex 2016;26:3977–90. https://doi.org/10.1093/cercor/bhw245.
[23] Schilberg L, Engelen T, ten Oever S, Schuhmann T, de Gelder B, de Graaf TA, et al. Phase of beta-frequency tACS over primary motor cortex modulates corticospinal excitability. Cortex 2018;103:142–52. https://doi.org/10.1016/j.cortex.2018.03.001.
[24] Khatoun A, Breukers J, Op de Beeck S, Nica IG, Aerts J-M, Seynaeve L, et al. Using high-amplitude and focused transcranial alternating current stimulation to entrain physiological tremor. Sci Rep 2018;8:8221. https://doi.org/10.1038/s41598-018-26013-3.
[25] Mehta AR, Brittain J-S, Brown P. The selective influence of rhythmic cortical versus cerebellar transcranial stimulation on human physiological tremor. J Neurosci 2014;34:7501–8. https://doi.org/10.1523/JNEUROSCI.0510-14.2014.
[26] Brittain J-S, Probert-Smith P, Aziz TZ, Brown P. Tremor suppression by rhythmic transcranial current stimulation. Curr Biol 2013;23:436–40. https://doi.org/10.1016/j.cub.2013.01.068.
[27] Muthuraman M, Raethjen J, Koirala N, Anwar AR, Mideksa KG, Elble R, et al. Cerebello-cortical network fingerprints differ between essential, Parkinson's and mimicked tremors. Brain 2018;141:1770–81. https://doi.org/10.1093/brain/awy098.
[28] Riecke L, Sack AT, Schroeder CE. Endogenous delta/theta sound-brain phase entrainment accelerates the buildup of auditory streaming. Curr Biol 2015;25:3196–201. https://doi.org/10.1016/j.cub.2015.10.045.
[29] Herrmann CS. Human EEG responses to 1-100 Hz flicker: resonance phenomena in visual cortex and their potential correlation to cognitive phenomena. Exp Brain Res 2001;137:346–53. https://doi.org/10.1007/s002210100682.
[30] Vossen A, Gross J, Thut G. Alpha power increase after transcranial alternating current stimulation at alpha frequency (α-tACS) reflects plastic changes rather than entrainment. Brain Stimul. 2015;8:499–508. https://doi.org/10.1016/j.brs.2014.12.004.
[31] Zaehle T, Rach S, Herrmann CS. Transcranial alternating current stimulation enhances individual alpha activity in human EEG. PloS One 2010;5:e13766. https://doi.org/10.1371/journal.pone.0013766.
[32] Laakso I, Hirata A. Computational analysis shows why transcranial alternating current stimulation induces retinal phosphenes. J Neural Eng 2013;10:046009. https://doi.org/10.1088/1741-2560/10/4/046009.
[33] Tort ABL, Komorowski R, Eichenbaum H, Kopell N. Measuring phase-amplitude coupling between neuronal oscillations of different frequencies. J Neurophysiol 2010;104:1195–210. https://doi.org/10.1152/jn.00106.2010.
[34] Wilsch A, Neuling T, Obleser J, Herrmann CS. Transcranial alternating current stimulation with speech envelopes modulates speech comprehension. Neuroimage 2018;172:766–74. https://doi.org/10.1016/j.neuroimage.2018.01.038.
[35] Pascual-Marqui RD. Discrete, 3D distributed, linear imaging methods of electric neuronal activity. Part 1: exact, zero error localization. 2007. p. 1–16. 07103341.
[36] Berens P. CircStat: a MATLAB toolbox for circular statistics. J Stat Software 2009;31:1–21.
[37] Izhikevich EM. Simple model of spiking neurons. IEEE Trans Neural Network 2003;14:1569–72. https://doi.org/10.1109/TNN.2003.820440.
[38] Izhikevich EM. Polychronization: computation with spikes. Neural Comput 2006;18:245–82. https://doi.org/10.1162/089976606775093882.
[39] Keitel C, Keitel A, Benwell CSY, Daube C, Thut G, Gross J. Stimulus-driven brain rhythms within the alpha band: the attentional-modulation conundrum. J Neurosci 2019;39:3119–29. https://doi.org/10.1523/JNEUROSCI.1633-18.2019.
[40] Notbohm A, Kurths J, Herrmann CS. Modification of brain oscillations via rhythmic light stimulation provides evidence for entrainment but not for superposition of event-related responses. Front Hum Neurosci 2016;10:10. https://doi.org/10.3389/fnhum.2016.00010.
[41] Zoefel B, ten Oever S, Sack AT. The involvement of endogenous neural oscillations in the processing of rhythmic input: more than a regular repetition of evoked neural responses. Front Neurosci 2018;12:1–13. https://doi.org/10.3389/fnins.2018.00095.
[42] Wischnewski M, Engelhardt M, Salehinejad MA, Schutter DJLG, Kuo MF, Nitsche MA. NMDA receptor-mediated motor cortex plasticity after 20 Hz transcranial alternating current stimulation. Cerebr Cortex 2019;29:2924–31. https://doi.org/10.1093/cercor/bhy160.
[43] Marshall L, Helgadóttir H, Mölle M, Born J. Boosting slow oscillations during sleep potentiates memory. Nature 2006;444:610–3. https://doi.org/10.1038/nature05278.
[44] Hanslmayr S, Matuschek J, Fellner M-C. Entrainment of prefrontal beta oscillations induces an endogenous echo and impairs memory formation. Curr Biol 2014;24:904–9. https://doi.org/10.1016/j.cub.2014.03.007.
[45] Halbleib A, Gratkowski M, Schwab K, Ligges C, Witte H, Haueisen J. Topographic analysis of engagement and disengagement of neural oscillators in photic driving. J Clin Neurophysiol 2012;29:33–41. https://doi.org/10.1097/WNP.0b013e318246ad6e.
[46] Stonkus R, Braun V, Kerlin JR, Volberg G, Hanslmayr S. Probing the causal role of prestimulus interregional synchrony for perceptual integration via tACS. Sci Rep 2016;6:32065.
[47] Ruhnau P, Neuling T, Fuscá M, Herrmann CS, Demarchi G, Weisz N. Eyes wide shut: transcranial alternating current stimulation drives alpha rhythm in a state dependent manner. Sci Rep 2016;6:27138. https://doi.org/10.1038/srep27138.
[48] Neuling T, Rach S, Herrmann CS. Orchestrating neuronal networks: sustained after-effects of transcranial alternating current stimulation depend upon brain states. Front Hum Neurosci 2013;7:161. https://doi.org/10.3389/fnhum.2013.00161.
[49] Alagapan S, Schmidt SL, Lefebvre J, Hadar E, Shin HW, Fröhlich F. Modulation of cortical oscillations by low-frequency direct cortical stimulation is state-dependent. PLoS Biol 2016;14:e1002424. https://doi.org/10.1371/journal.pbio.1002424.
[50] Asamoah B, Khatoun A, Mc Laughlin M. tACS motor system effects can be caused by transcutaneous stimulation of peripheral nerves. Nat Commun 2019;10:266. https://doi.org/10.1038/s41467-018-08183-w.
[51] Vieira PG, Krause MR, Pack CC. tACS entrains neural activity while somatosensory input is blocked. BioRxiv 2019:691022. https://doi.org/10.1101/691022.
[52] van der Groen O, Wenderoth N. Transcranial random noise stimulation of visual cortex: stochastic resonance enhances central mechanisms of perception. J Neurosci 2016;36:5289–98. https://doi.org/10.1523/JNEUROSCI.4519-15.2016.
[53] Ozen S, Sirota A, Belluscio MA, Anastassiou CA, Stark E, Koch C, et al. Transcranial electric stimulation entrains cortical neuronal populations in rats. J Neurosci 2010;30:11476–85. https://doi.org/10.1523/JNEUROSCI.5252-09.2010.
[54] Cabral-Calderin Y, Anne Weinrich C, Schmidt-Samoa C, Poland E, Dechent P, Bähr M, et al. Transcranial alternating current stimulation affects the BOLD signal in a frequency and task-dependent manner. Hum Brain Mapp 2016;37:94–121. https://doi.org/10.1002/hbm.23016.
[55] Chai Y, Sheng J, Bandettini PA, Gao J-H. Frequency-dependent tACS modulation of BOLD signal during rhythmic visual stimulation. Hum Brain Mapp 2018;39:2111–20. https://doi.org/10.1002/hbm.23990.
[56] Herring JD, Esterer S, Marshall TR, Jensen O, Bergmann TO. Low-frequency alternating current stimulation rhythmically suppresses gamma-band oscillations and impairs perceptual performance. Neuroimage 2019;184:440–9. https://doi.org/10.1016/j.neuroimage.2018.09.047.
[57] Morgan ST, Hansen JC, Hillyard SA, Posner M. Selective attention to stimulus location modulates the steady-state visual evoked potential. Proc Natl Acad Sci Unit States Am 1996;93:4770–4.
[58] Notbohm A, Herrmann CS. Flicker regularity is crucial for entrainment of alpha oscillations. Front Hum Neurosci 2016;10:503. https://doi.org/10.3389/fnhum.2016.00503.
[59] Ruhnau P, Keitel C, Lithari C, Weisz N, Neuling T. Flicker-driven responses in visual cortex change during matched-frequency transcranial alternating current stimulation. Front Hum Neurosci 2016;10:184. https://doi.org/10.3389/fnhum.2016.00184.